FCS-MPC and Observer Design in the dq Synchronous Frame: An Experimental Validation

Eduardo Zafra
Universidad de Sevilla
Seville, Spain,
ezafra1@us.es

Sergio Vazquez
Universidad de Sevilla
Seville, Spain,
sergi@us.es

Tobias Geyer
ABB Corporate Research
5405 Baden-Dättwil, Switzerland,
t.geyer@ieee.org

Ricardo P. Aguilera
University of Technology Sydney
Sydney, NSW 2007, Australia,
raguilera@ieee.org

Leopoldo G. Franquelo
Universidad de Sevilla and Harbin Institute of Technology,
Seville, Spain and Harbin, China,
lgfranquelo@us.es

Jose I. Leon
Universidad de Sevilla and Harbin Institute of Technology,
Seville, Spain and Harbin, China,
jileon@us.es

***Abstract*—The addition of an output LC filter to a voltage source inverter (VSI) allows the generation of high-quality output voltages with reduced harmonic distortion content. For this reason, this topology is widely used for uninterruptible power supply (UPS) applications. To control this system, finite control set model predictive control (FCS-MPC) has been assessed in previous research with promising results. In this paper, the dq-synchronous reference frame (dq-SRF) formulation of FCS-MPC and a state observer for an UPS system are presented and experimentally validated. The advantage of this proposal lies in the simplification of the observer design by considering a deadbeat observer along with the addition of a low-pass filter. In this way, the observer bandwidth is simply determined by the cutoff frequency of the low-pass filter. Simulation and experimental results are compared to assess the performance of the proposed solution.**

I. Introduction

UNINTERRUPTIBLE power supply (UPS) is a well-known application in industry. They are capable of delivering a continuous and reliable electrical power to sensitive and critical loads, such as medical equipment, telecommunication systems or data centers [1]. Due to its usage to supply critical loads, one of the main challenges for a UPS application is to achieve a reduced low order harmonic content in the output voltage according to grid standards [2]. This is the reason why an LC filter is included in the output of the voltage source inverter (VSI). Thus, a great part of the output voltage harmonic components can be removed. Nonetheless, the addition of this output filter comes at the expense of a greater complexity for the system model and the control design. This comes from the fact that besides the output inverter current, more states are added to the model and in case of not measuring them, they need to be estimated [3], [4].

Out of the several proposed techniques to approach the control of these systems, model predictive control (MPC), and in particular finite control set MPC (FCS-MPC), has garnered significant interest in recent years. Although there are still some open issues, generally FCS-MPC presents a fast dynamic response and the capability to simultaneously consider multiple control objectives, system constraints and nonlinearities [5]–[9].

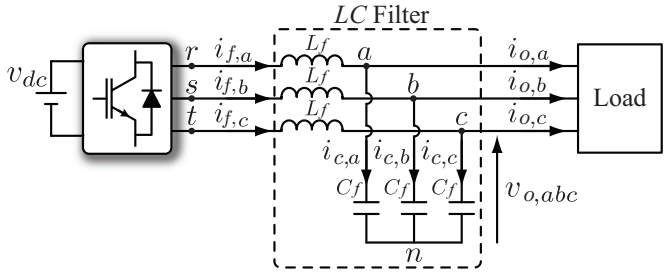

Fig. 1. Three-phase inverter with output LC filter circuit.

In order to design an FCS-MPC strategy, a model of the system is required to calculate predictions of the system state evolution up to a certain prediction horizon length. For the UPS application, models for the dq and $\alpha\beta$ reference frames have been developed in [3], [10], [11]. In these works, FCS-MPC strategies, with the inclusion of a Luenberger observer [12] for the estimation of the output currents, were proposed and analyzed. Particularly, in [11] the performance of these strategies is assessed and compared with simulation results. Basically, once both controllers are formulated and the cost function is defined, the only degree of freedom left to influence the overall closed-loop performance is the observer gain matrix. Therefore, the main goal is to find a tuning procedure for the observer that allows one to perform a fair comparison between both controllers. It is demonstrated in [11] that this could be achieved by obtaining an observer gain matrix with a specific structure. One way to satisfy this structure condition is by considering a deadbeat observer. Thus, the observer gain matrix can be easily designed using a pole-placement technique by positioning the observer poles in the origin of the z-plane. However, a deadbeat observer has the disadvantage of providing noisy system state estimates with high frequency noise. Therefore, a low-pass filter (LPF) is added to obtain a

TABLE I
SYSTEM VARIABLES AND PARAMETERS

Variable	Description
$v_{i,dq}$	VSI output voltage
$v_{o,dq}$	Output filter capacitor voltage
$v^*_{o,dq}$	Output filter capacitor voltage reference
$i_{f,dq}$	Output filter inductor current
$i_{o,dq}$	Output load current
L_f	Output filter inductor
C_f	Output filter capacitor
v_{dc}	DC-link voltage
ω	Angular frequency of the output reference voltage

reduced noise in the state estimates. This technique simplifies the observer design since the overall observer bandwidth is determined by the low-pass filter bandwidth.

In this paper, an experimental validation of these results is presented to verify the performance of the proposed controller in the dq-synchronous reference frame (dq-SRF). Expressions for the prediction model, cost function and state variables are presented in Section II. Section III offers a first set of experiments implementing the proposed design. Section IV is dedicated to the design of a low-pass filter for the current estimate. Final experimental results of the overall proposal are presented in Section V.

II. SYSTEM MODEL AND OBSERVER

This section is dedicated to the modeling of the system and design of the state variables observer. In Fig. 1, the electric circuit of the inverter and the LC filter is represented. In Table I, all system variables and parameters are listed.

To design an FCS-MPC strategy, it is firstly required to obtain a discrete-time mathematical model that allows the control algorithm to compute predictions of the system state variables for the next sampling instant. With these predictions, a cost function can be computed and minimized in order to choose the optimal switching state for the next sampling interval, i.e., the input combination that minimizes the cost function. The formulation of the cost function considers the control targets. In this particular case, the control target is the regulation of the filter output voltages to an imposed reference. Therefore, the cost function is chosen as the quadratic euclidean norm of the error between the output voltage prediction and its desired reference at the sampling instant $k+2$:

$$g = \|v^*_{o,dq}(k+2) - v_{o,dq}(k+2)\|_2^2 \tag{1}$$

The system dynamic equations are derived in [3], [10], [11]. These mathematical models can be expressed in their state-space representation with the following structure:

$$\frac{dx_{dq}}{dt} = Ax_{dq} + Bu_{dq} + A_d w_{dq} \tag{2}$$

$$y_{dq} = Cx_{dq} \tag{3}$$

where:

$$x_{dq} = y_{dq} = \begin{bmatrix} i_{f,dq} \\ v_{o,dq} \end{bmatrix}, u_{dq} = \begin{bmatrix} v_{i,dq} \\ Z_2 \end{bmatrix}, w_{dq} = \begin{bmatrix} Z_2 \\ i_{o,dq} \end{bmatrix},$$

$$A = \begin{bmatrix} -J\omega & -\frac{1}{L_f} I_2 \\ \frac{1}{C_f} I_2 & -J\omega \end{bmatrix}, B = \begin{bmatrix} \frac{1}{L_f} I_2 \\ O_2 \end{bmatrix}, A_d = \begin{bmatrix} O_2 \\ -\frac{1}{C_f} I_2 \end{bmatrix},$$

$$C = \begin{bmatrix} I_2 & O_2 \\ O_2 & I_2 \end{bmatrix}, J = \begin{bmatrix} 0 & -1 \\ 1 & 0 \end{bmatrix},$$

and $v_{i,dq}, v_{o,dq}, i_{f,dq}, i_{o,dq}, Z_2 \in \mathbb{R}^2$. Here, I_2 is the identity matrix and O_2 a null matrix, both are of 2×2 dimension. Z_2 is a null vector. Also, $v_{i,dq} = v_{dc}\, S_{dq}$, where $S_{dq} \in \mathbb{R}^2$ is the switching state of the inverter, expressed in the dq-SRF.

These equations define the system prediction model. For this application, it is assumed that measurements of the output currents are not available. Therefore, they appear in the model as an external disturbance w_{dq}. In order to take into account this disturbance, an observer can be used to estimate the output currents. We will use the full-order state observer formulation proposed in [12]. Basically, this observer is capable of obtaining a state vector estimate through the instantaneous information of the system inputs and outputs. According to this, it is necessary to reformulate the problem so that the output currents can be considered a state variable of the system. We can assume a certain dynamic behavior for these variables, and extend the state variables vector, which can be rewritten as: $x_{e,dq} = \begin{bmatrix} i^T_{f,dq} & v^T_{o,dq} & i^T_{o,dq} \end{bmatrix}^T$. Assuming a constant dynamic for the output currents in the dq-SRF, the state-space model for this augmented system can be obtained by merely reorganizing the equations in (2) (3). Note that the output of this augmented system ($y_{e,dq}$) is equal to the output of the original system (y_{dq}).

$$\frac{dx_{e,dq}}{dt} = A_e x_{e,dq} + B_e u_{dq} \tag{4}$$

$$y_{e,dq} = C_e x_{e,dq} \tag{5}$$

where:

$$A_e = \begin{bmatrix} -J\omega & -\frac{1}{L_f} I_2 & O_2 \\ \frac{1}{C_f} I_2 & -J\omega & -\frac{1}{C_f} I_2 \\ O_2 & O_2 & O_2 \end{bmatrix}, B_e = \begin{bmatrix} \frac{1}{L_f} I_2 \\ O_2 \\ O_2 \end{bmatrix},$$

$$C_e = \begin{bmatrix} I_2 & O_2 & O_2 \\ O_2 & I_2 & O_2 \end{bmatrix} \tag{6}$$

are the extended system matrices in dq. The corresponding Luenberger observer system is formulated in (7) (8):

$$\frac{d\hat{x}_{e,dq}}{dt} = A_e \hat{x}_{e,dq} + B_e u_{dq} + G_{dq}(y_{dq} - \hat{y}_{e,dq}) \tag{7}$$

$$\hat{y}_{e,dq} = C_e \hat{x}_{e,dq} \tag{8}$$

In these equations, $\hat{x}_{e,dq} = \begin{bmatrix} \hat{i}^T_{f,dq} & \hat{v}^T_{o,dq} & \hat{i}^T_{o,dq} \end{bmatrix}^T$ is the estimated augmented state vector in the dq-SRF. From this vector, only the current estimate is fed into the system prediction model. Thus, $\hat{y}_{e,dq}$ is the output of the observer and G_{dq} is the observer gain matrix.

The equation in (7) can be written in a compact form as:

$$\frac{d\hat{x}_{e,dq}}{dt} = \underbrace{[A_e - G_{dq}\, C_e]}_{A_{obs}}\, \hat{x}_{e,dq} + \underbrace{[B_e,\ G_{dq}]}_{B_{obs}} \underbrace{\begin{bmatrix} v_{i,dq} \\ i_{f,dq} \\ v_{o,dq} \end{bmatrix}}_{u_{obs,dq}} \tag{9}$$

The observer gain matrix has an important influence on the overall (FCS-MPC plus observer) closed-loop performance, as a wrong estimate of the output currents can cause a poor behavior of the controller. Generally, higher values for the gain matrix provide a faster dynamic response for the estimate but cause a noisier output, which may degrade the controller performance. Therefore, a trade-off must be achieved when tuning these parameters. The values of the gain matrix are chosen by solving a pole placement problem where the poles of A_{obs} are placed in order to achieve a required performance. In [11], a deadbeat strategy was followed to tune the gain matrix of the observer. This tuning strategy rendered good results in simulations while greatly simplified the tuning process of the observer, as all the poles are now placed in the origin of the z-plane, and therefore, there is no need to individually tweak their positions in the z-plane.

III. First Experimental Validations

In this section, the dq-SRF controller and observer design proposed in [11] is experimentally assessed. To do that, tests are carried out on a VSI with output LC filter prototype. A three-phase linear load consisting of a resistor and an inductor is connected in series to the system output.

To implement the digital control, a Xilinx Zynq-7000 All Programmable System on Chip (APSoC), running on a Pynq-Z1 evaluation kit is used [13]. This system is composed of a dual-core ARM Cortex-A9 processing system that can run at up to 667 MHz and an Artix-7 FPGA based programmable logic unit. For this application, we use the FPGA to handle the timing of the devices, providing the interrupt signals for the processors, and the firing pulses for the power converter. The 12-bit ADC present in the programmable logic side of the device is also utilized for measurements. For the processing system, a configuration called "Asymmetric Multiprocessing" is implemented [14]. This allows one to use both cores independently. In particular, we use this characteristic so that one of the cores runs a Linux operating system that executes an application that handles all the external communications through the TCP/IP protocol, while the other core executes a baremetal application where the control algorithm is executed.

The main experimental prototype parameters can be found in Table II. To assess the steady state behaviour of the controller, the total harmonic distortion (THD) of the generated output voltage is measured with a Fluke 434 Series II power quality analyser [15], which measures the harmonic content up to the 50^{th} harmonic. Also, a load step change is performed in order to assess the dynamic response of both the FCS-MPC and the designed observer. In Fig. 2, the results obtained through simulation are presented. Experimental results are shown in Fig. 3.

TABLE II
Parameters for Experiments

Parameters	Value
DC-Link Voltage [V]	700
Reference Phase Voltage Amplitude [Vph-n]	325
Filter Capacitor [μF]	50
Filter Inductor [mH]	2
Load Resistance [Ω]	30
Load Inductor [mH]	20
Sampling Interval [μs]	40
Reference frequency for electrical signals [Hz]	50
Load connection time [s]	≈ 0.012

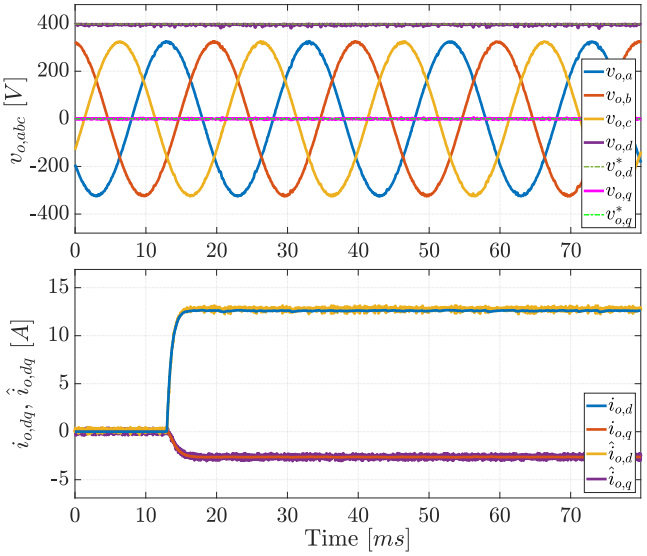

Fig. 2. Simulation results. Top: Generated output voltages. Bottom: Current estimates.

As it can be seen, simulation and experimental results greatly differ. Measuring the output voltage with the referenced power quality analyser, the resulting THD is 2.4%. Computing the THD for the simulation up to the same harmonic, the result is 0.72%. This means that the steady state controller behaviour is very poor when implemented in a real equipment. The explanation for this can be found in the plot of the currents estimates. The problem is that the observer estimates are very noisy. This is due to the fact that the aggressive (high-bandwith) behaviour of deadbeat observer is acting as an amplifier of all the measurement noise. It is apparent that a deadbeat tuning, while simple and performing well in simulations, is not a good solution when tested in a real power converter device.

IV. Low-Pass Filter

In order to address the problem, the noisy output of the deadbeat observer will be filtered with a low-pass filter. The idea is to preserve the simplicity of the deadbeat observer and check whether the addition of a simple low-pass filter to

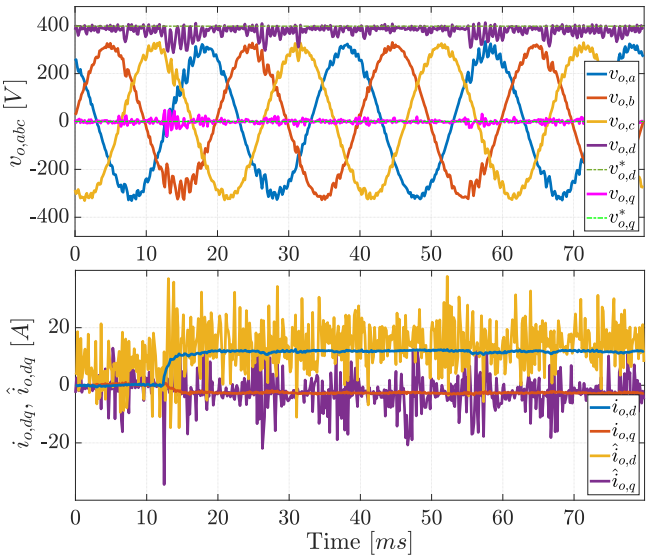

Fig. 3. Experimental results. Top: Generated output voltages. Bottom: Estimated currents.

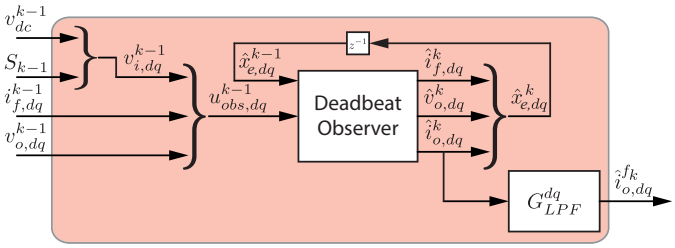

Fig. 4. Block diagram of the observer after the low-pass filter addition.

remove high frequency noise from the output current estimate is sufficient to bring experimental results closer to the ones obtained in simulation.

The Laplace-domain transfer function for a first order low-pass filter with an unity filter gain is:

$$H(s) = \frac{1}{\tau s + 1}, \tag{10}$$

where τ is the time constant of the filter, which can be expressed in function of the cutoff frequency (f_c) of the filter as:

$$\tau = \frac{1}{2\pi f_c} \tag{11}$$

To obtain the filtered observer output in dq, the following equation is used:

$$\hat{i}^f_{o,dq} = \begin{bmatrix} H(s) & 0 \\ 0 & H(s) \end{bmatrix} \hat{i}_{o,dq}, \tag{12}$$

where $\hat{i}^f_{o,dq}$ is the filtered observer output.

If this transfer function is discretized by means of any method, like Forward-Euler, and then implemented in the control hardware, its output will reduce high frequency noise in the estimate of the output current. With this method, the

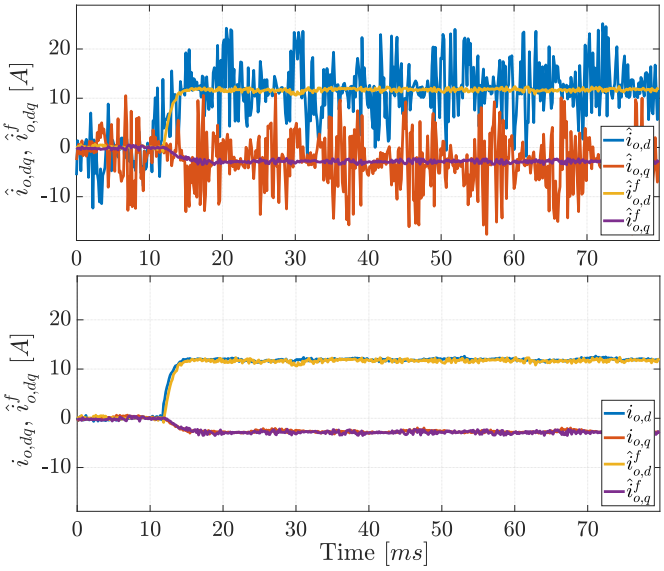

Fig. 5. Low-pass filter results. Top: Estimate of currents and filtered currents. Bottom: Real currents and filtered currents. Cutoff frequency is configured at 500 Hz.

observer structure can be summarized in the block diagram shown in Fig. 4. The main advantage of this strategy is that the observer tuning remains simple. Since a first order filter was chosen, the cutoff frequency is the only additional parameter. This parameter acts as a limiter for the observer bandwidth. In this way, the bandwidth of the overall observer structure (observer plus LPF) can be easily imposed, avoiding the need to tweak the placement of the observer poles, which is not a straightforward process. Also, the fact that a first order filter was chosen means that the generated computational overhead is very small, compared to more complex filter expressions available in the literature.

It is still necessary to investigate whether the proposed control strategy is capable of providing an acceptable performance. First, the isolated behaviour of the filter is assessed. In Fig. 5, the input and output of the filter are represented for a cutoff frequency of 500 Hz. In this experiment, the observer output is filtered without feeding this information to the controller, in order to assess the low-pass filter noise reduction performance. As can be seen in the top subfigure, the noise present in the current estimate has been almost completely removed by the LPF. In the bottom subfigure, it can be noticed that the filtered current estimates are close to the real currents. In section V, the performance of this new observer structure along with the controller will be assessed.

V. Final Experimental Validations

This section is dedicated to the final validation of the proposed control strategy, with the inclusion of the observer structure proposed in section IV. In these new experiments, the effect of the cutoff frequency of the LPF is tested by presenting experiments with different values for this tuning parameter.

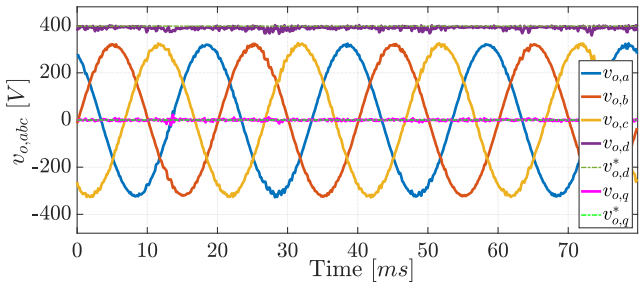

(a) Cutoff frequency $f_c = 100$ Hz.

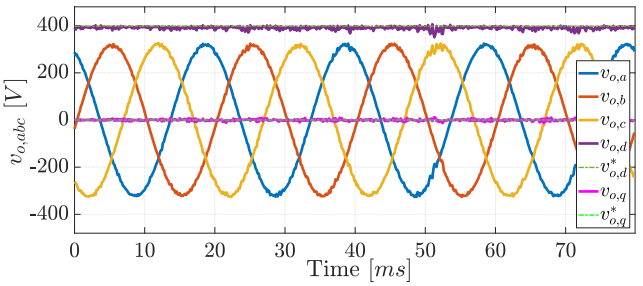

(b) Cutoff frequency $f_c = 600$ Hz.

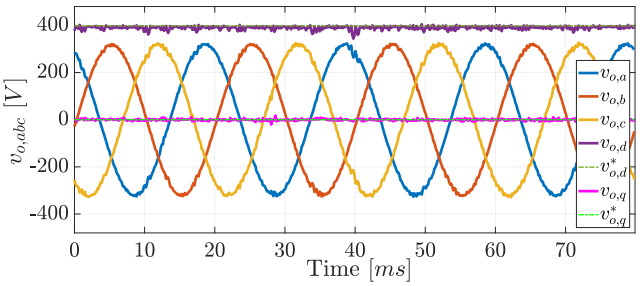

(c) Cutoff frequency $f_c = 1000$ Hz.

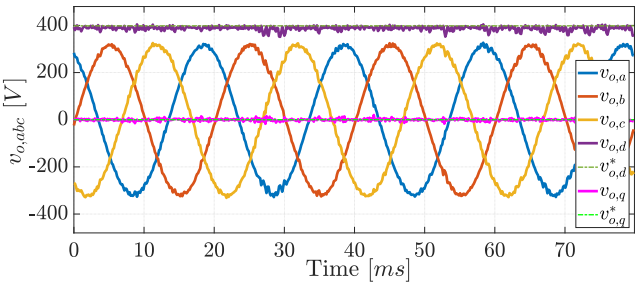

(d) Cutoff frequency $f_c = 3500$ Hz.

Fig. 6. Experimental output voltages with the new observer structure. Generated output voltages for different cutoff frequencies.

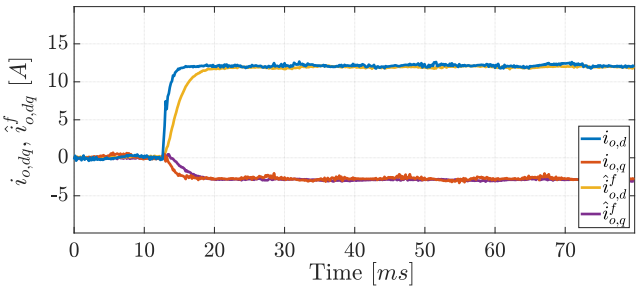

(a) Cutoff frequency $f_c = 100$ Hz.

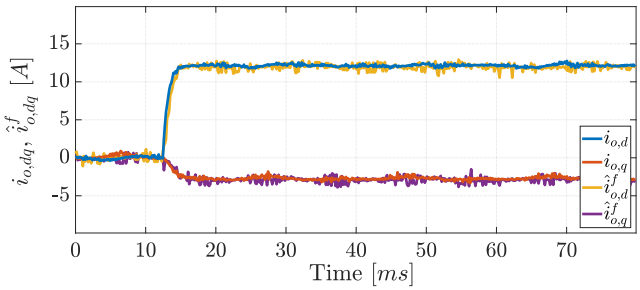

(b) Cutoff frequency $f_c = 600$ Hz.

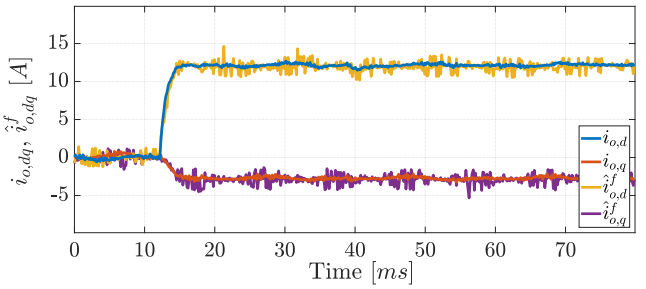

(c) Cutoff frequency $f_c = 1000$ Hz.

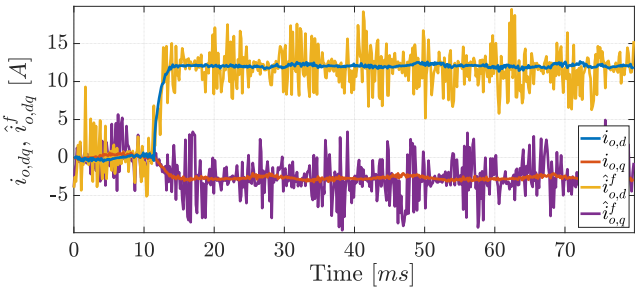

(d) Cutoff frequency $f_c = 3500$ Hz.

Fig. 7. Experimental output currents with the new observer structure. Currents estimates for different cutoff frequencies.

The output voltages are shown in Fig. 6. The current estimates are shown along with the real currents in Fig. 7. As can be seen in this figure, lowering the cutoff frequency of the filter allows the proposed observer structure to greatly reduce the noise content in the estimates. However, the resulting closed-loop transient response becomes slower. To assess the steady-state performance, the THD of the output voltage is measured. The resulting THDs for all the experiments and simulations are summarized in Table III. Here, the average switching frequency (F_{sw}^{avg}) is also presented.

From the results, it can be noticed that when the filter is tuned at 100 Hz, the appreciable delay in the filtered current response translates to a small degradation of the voltage reference tracking when the load step happens. This effect

TABLE III
THD RESULTS

Case	THD [%]	F_{sw}^{avg} [kHz]
Simulation	0.72	6.22
Experiment without LPF	2.4	4.69
Experiment with LPF, $f_c = 100$ Hz	0.9	5.24
Experiment with LPF, $f_c = 600$ Hz	1.0	5.41
Experiment with LPF, $f_c = 1000$ Hz	1.0	5.38
Experiment with LPF, $f_c = 3500$ Hz	1.5	5.10

disappears in the other subfigures of Fig. 6, as the estimates become closer to the real currents. As the cutoff frequency becomes higher, noise starts to appear in the estimates again. For $f_c = 3500$ Hz, the steady state performance is noticeable worsened as the estimation noise becomes too high. Finally, for this particular system, it has be found that a cutoff frequency at around 600 Hz provides a good tradeoff between the closed-loop dynamic response and the steady-state performance of the overall proposed predictive control strategy.

VI. CONCLUSION

An experimental validation of the FCS-MPC for a UPS application proposed in [11] has been carried out. The implementation of this control method has been performed in a Pynq Z-1 evaluation board for the Xilinx Zynq-7000 APSoC. First, it was found that the observer design proposed in [11] was too aggressive (high bandwidth), providing noisy estimates when tested in a real implementation. Contrary to the obtained simulation results, the observer provided a poor estimate of the output currents which translated into a deficient steady state performance of the resulting closed-loop in terms of THD.

In order to solve this, a digital low-pass filter was applied to mitigate the noise that was present in the estimated output current. The new observer structure combines the advantage of a simple observer design based on deadbeat tuning with a reduced noise in the estimated variables. This fact is checked through extensive experimental results, which validate the proposed design of the overall predictive control strategy for a UPS.

ACKNOWLEDGMENT

The authors gratefully acknowledge the financial support provided by Spanish Ministry of Economy and Competitivity under the project TEC2016-78430-R and EU H2020 under the grant agreement id: 821381. Sections III and V were made possible by NPRP 9-310-2-134 from the Qatar National Research Fund (a member of Qatar Foundation). This research was also funded in part by the Australian Government through the Australian Research Council (Discovery Project No. DPDP180100129). The statements made herein are solely the responsibility of the authors.

REFERENCES

[1] J. M. Guerrero, L. Garcia De Vicuna, and J. Uceda, "Uninterruptible power supply systems provide protection," *IEEE Industrial Electronics Magazine*, vol. 1, DOI 10.1109/MIE.2007.357184, no. 1, pp. 28–38, Spring 2007.

[2] IEC standard for uninterruptible power systems (UPS) - part 3. [IEC62040-3 2011, no 2, Mar 2011].

[3] P. Cortes, G. Ortiz, J. I. Yuz, J. Rodriguez, S. Vazquez, and L. G. Franquelo, "Model predictive control of an inverter with output LC filter for ups applications," *IEEE Transactions on Industrial Electronics*, vol. 56, DOI 10.1109/TIE.2009.2015750, no. 6, pp. 1875–1883, Jun. 2009.

[4] B. Majmunovic, T. Dragicevic, and F. Blaabjerg, "Multi objective modulated model predictive control of stand-alone voltage source converters," *IEEE Journal of Emerging and Selected Topics in Power Electronics*, DOI 10.1109/JESTPE.2019.2925603, pp. 1–1, 2019.

[5] S. Vazquez, J. Rodriguez, M. Rivera, L. G. Franquelo, and M. Norambuena, "Model predictive control for power converters and drives: Advances and trends," *IEEE Transactions on Industrial Electronics*, vol. 64, DOI 10.1109/TIE.2016.2625238, no. 2, pp. 935–947, Feb. 2017.

[6] S. Vazquez, J. I. Leon, L. G. Franquelo, J. Rodriguez, H. A. Young, A. Marquez, and P. Zanchetta, "Model predictive control: A review of its applications in power electronics," *IEEE Industrial Electronics Magazine*, vol. 8, DOI 10.1109/MIE.2013.2290138, no. 1, pp. 16–31, Mar. 2014.

[7] P. Karamanakos and T. Geyer, "Guidelines for the design of finite control set model predictive controllers," *IEEE Transactions on Power Electronics*, DOI 10.1109/TPEL.2019.2954357, pp. 1–1, 2019.

[8] C. Bordons and C. Montero, "Basic principles of mpc for power converters: Bridging the gap between theory and practice," *IEEE Industrial Electronics Magazine*, vol. 9, DOI 10.1109/MIE.2014.2356600, no. 3, pp. 31–43, Sep. 2015.

[9] S. Vazquez, P. Acuna, R. P. Aguilera, J. Pou, J. I. Leon, and L. G. Franquelo, "Dc-link voltage balancing strategy based on optimal switching sequences model predictive control for single-phase h-npc converters," *IEEE Transactions on Industrial Electronics*, DOI 10.1109/TIE.2019.2941131, pp. 1–1, 2019.

[10] S. Vazquez, A. Marquez, J. I. Leon, L. G. Franquelo, and T. Geyer, "FCS-MPC and observer design for a VSI with output LC filter and sinusoidal output currents," in *2017 11th IEEE International Conference on Compatibility, Power Electronics and Power Engineering (CPE-POWERENG)*, DOI 10.1109/CPE.2017.7915254, pp. 677–682, Apr. 2017.

[11] E. Zafra, S. Vazquez, T. Geyer, F. J. Gonzalez, A. Marquez, J. I. Leon, and L. G. Franquelo, "Finite control set model predictive control with an output current observer in the dq-synchronous reference frame for an uninterruptible power supply system," in *2019 13th IEEE International Conference on Compatibility, Power Electronics and Power Engineering (CPE-POWERENG)*, Apr. 2019.

[12] D. Luenberger, "An introduction to observers," *IEEE Transactions on Automatic Control*, vol. 16, DOI 10.1109/TAC.1971.1099826, no. 6, pp. 596–602, Dec. 1971.

[13] PYNQ-Z1 Reference Manual. https://reference.digilentinc.com/reference/programmable-logic/pynq-z1/reference-manual. [Online - Accessed January 2020].

[14] Simple AMP running linux and bare-metal system on both zynq SoC processors. https://www.xilinx.com/support/documentation/application_notes/xapp1078-amp-linux-bare-metal.pdf. [Online - Accessed January 2019].

[15] Fluke 434 Series II. https://www.fluke.com/en-us/product/electrical-testing/power-quality-analyzers/three-phase-power-quality-meters/fluke-434-series-ii-basic. [Online - Accessed January 2020].